analytical chemistry

pubs.acs.org/ac
Article

Label-Free Raman Spectroscopy for Assessing Purity and Maturation of hiPSC-Derived Cardiac Tissue

Junjun Li,*,○ Menglu Li,○ Yasunori Nawa, Yuting Liu, Kazuki Bando, Ying Hua, Lifu Sun, Satoshi Fujita, Yoshiki Sawa, Katsumasa Fujita,* and Li Liu*

Cite This: *Anal. Chem.* 2024, 96, 15765−15772
Read Online

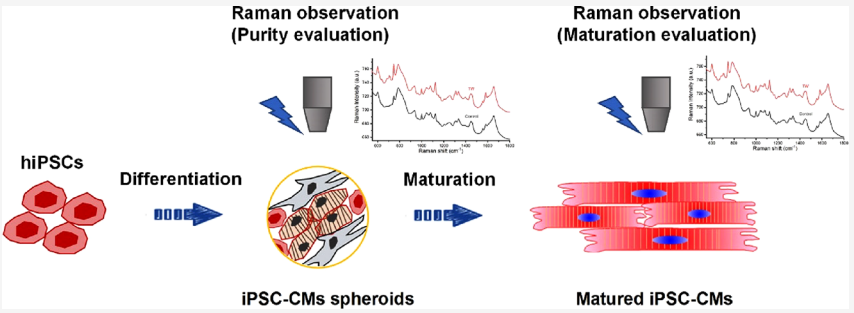

ABSTRACT: I. Background: Human induced pluripotent stem cell (hiPSC) derived cardiomyocytes (CMs) have been utilized in drug toxicity evaluation, drug discovery, and treating heart failure patients, showing substantial effects. Ensuring the quality, purity, and maturation of hiPSC-CMs during large-scale production is crucial. There is a growing demand for a novel method to characterize cell molecular profiles without labels and without causing damage. II. Methods: In this study, we employed label-free Raman microscopy to evaluate hiPSC-derived CMs. The study involved the characterization of cell molecular profiles without labels and without causing damage. The correlation between Raman spectroscopy of specific components, such as cytochrome *c* and myoglobin, and CM purity and maturation following hiPSC differentiation was investigated. Additionally, the validation of this correlation was performed by assessing mixtures of commercially available CMs (iCell cardiomyocytes2) and fibroblasts at various ratios as well as hiPSC-derived CMs with different efficiencies. Furthermore, CMs were matured using rapid pacing of traveling waves, and the Raman profiles of matured CMs were compared to those of immature ones. III. Results: Raman spectroscopy indicated that the cytochrome *c* and myoglobin showed correlation with the purity and maturation of CMs following differentiation of hiPSCs. This correlation was validated through experiments involving different CM-fibroblast mixtures and hiPSC-derived CMs with varying efficiencies. Moreover, matured CMs exhibited markedly different Raman profiles compared to immature ones, indicating the potential of Raman imaging as a tool for assessing CM maturation. IV. Conclusions: We discovered that Raman spectroscopy of certain components, such as cytochrome *c* and myoglobin, correlates with the CM purity and maturation following hiPSC differentiation. The findings of this study highlight the potential of label-free Raman microscopy as a nondestructive, high-content, and time-efficient method for quality control of hiPSC-derived CMs. This approach could significantly contribute to ensuring the quality and maturity of hiPSC-CMs for various applications in drug discovery and regenerative medicine.

INTRODUCTION

Cardiovascular disease remains the primary cause of global mortality. Human induced pluripotent stem cell (hiPSC)-derived cardiomyocytes (CMs) hold promise for heart failure treatment. Our group conducted pioneering allogeneic iPSC-CMs transplantation, affirming its efficacy and safety in multiple patients.[1,2,3,4] On the other hand, using human cardiomyocytes instead of animal experiments for drug toxicity testing and screening drugs for heart disease treatment is considered to have broader application prospects.[5] Quality control is paramount for large-scale hiPSC-CM production, focusing on parameters such as CM purity and maturation. Purity may be compromised by non-CMs, including residual iPSCs, potentially leading to teratoma formation post-transplantation. Evaluating CM maturity is crucial for assessing therapeutic efficacy post-transplantation and obtaining a more accurate response to drugs.[6] Current gold-standard molecular biology methods, such as flow cytometry and immunostaining, often induce cell damage during fixation.

Received: July 24, 2024
Revised: August 5, 2024
Accepted: September 6, 2024
Published: September 18, 2024

https://doi.org/10.1021/acs.analchem.4c03871
Anal. Chem. 2024, 96, 15765−15772

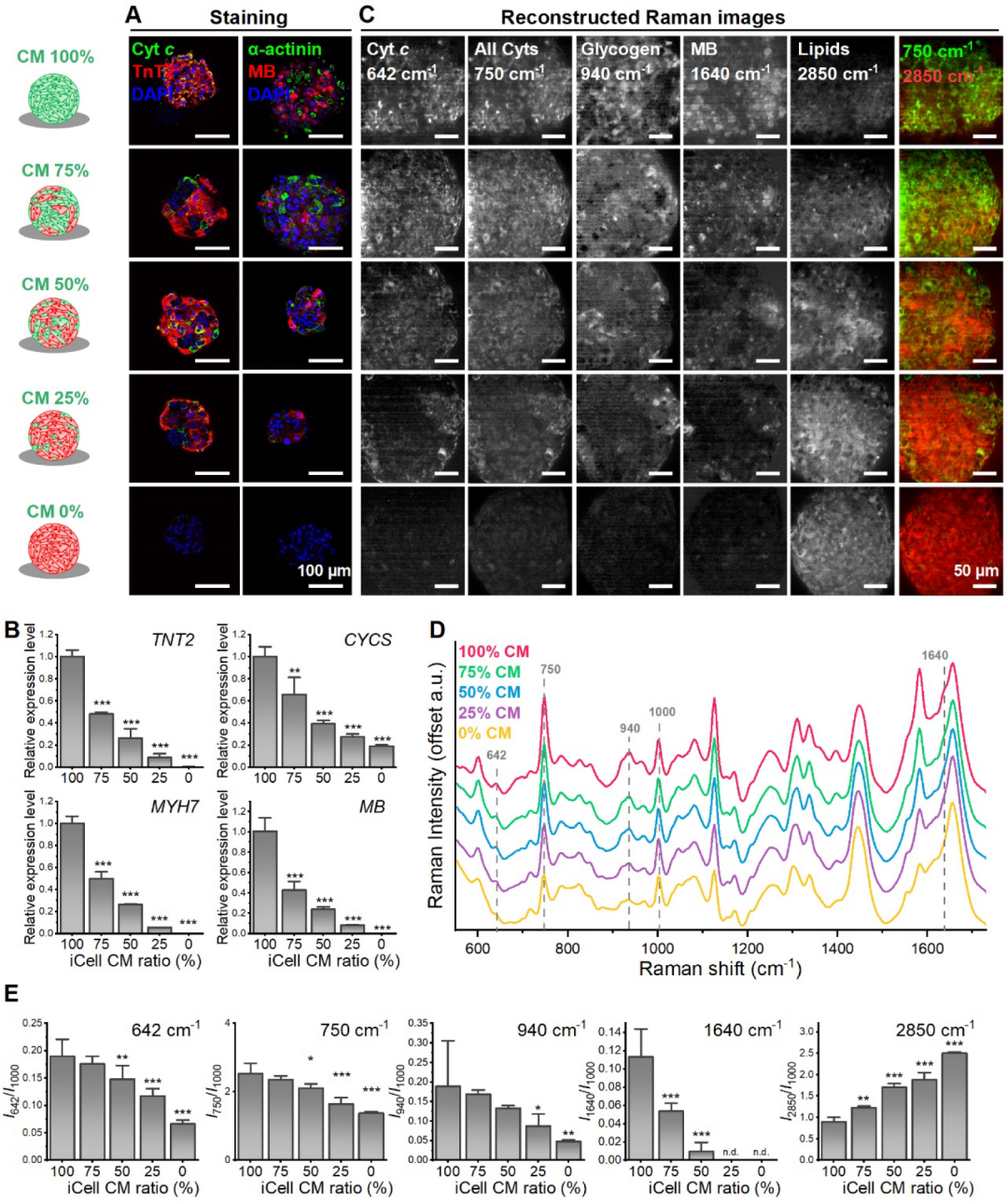

Figure 1. Raman observation on mixture of iCell with fibroblast. (A) Representative confocal images of iCell/fibroblast spheroid with different mixing ratio on day 3. The spheroids were stained with anti-TnT2, anti-cytochrome *c* (Cyt c), anti-α-actinin, anti-myoglobin (anti-MB), and DAPI. (B) Relative gene expression of *TnT2*, cytochrome *c* (*CYCS*), β-Myosin Heavy Chain (*MYH7*), myoglobin (*MB*) (Mean ± SD, $n = 3$ biologically independent samples, $^{**}p < 0.01$, $^{***}p < 0.001$). (C) Reconstructed Raman images at 642, 750, 940, 1,640, and 2,850 cm^{-1}. (D) Comparison of average Raman signal for iCell/fibroblast spheroid with different mixing ratios. (E) Quantitative analysis of the Raman intensity at 642, 750, 940, 1,640, and 2,850 cm^{-1} (mean ± SD, $n = 3$ biologically independent samples, $^{*}p < 0.05$, $^{**}p < 0.01$, $^{***}p < 0.001$).

The prevailing approach for CM preparation involves 3D differentiation protocols. Despite lacking superior alternatives to flow cytometry and genetic analysis, it is imperative to dissociate 3D spheroids into single cells for evaluation, although this may impact cell viability due to stress. There is a pressing need for a novel, nondestructive, and label-free technology to assess cells or 3D spheroid without dissociation, offering an alternative to traditional molecular biology assessments.

Raman microscopy is a potent, label-free, and nondestructive tool capable of monitoring live tissue based on the chemically specific vibrations of intrinsic cellular biomolecules.[7−9] It has been utilized to identify various cellular phenomena such as the cell death stage in apoptotic cells,[10] the stages of tumorigenesis,[11] and the developmental stages of hiPSC-derived neurons.[12] Furthermore, the accumulation of functional molecules in hepatocytes derived from hiPSCs during differentiation and maturation has been observed.[8]

A previous study demonstrated that Raman spectroscopy can distinguish CMs from the surrounding fibrotic area in a rat heart[7] and non-CMs in culture dish,[13] suggesting its potential

https://doi.org/10.1021/acs.analchem.4c03871
Anal. Chem. 2024, 96, 15765−15772

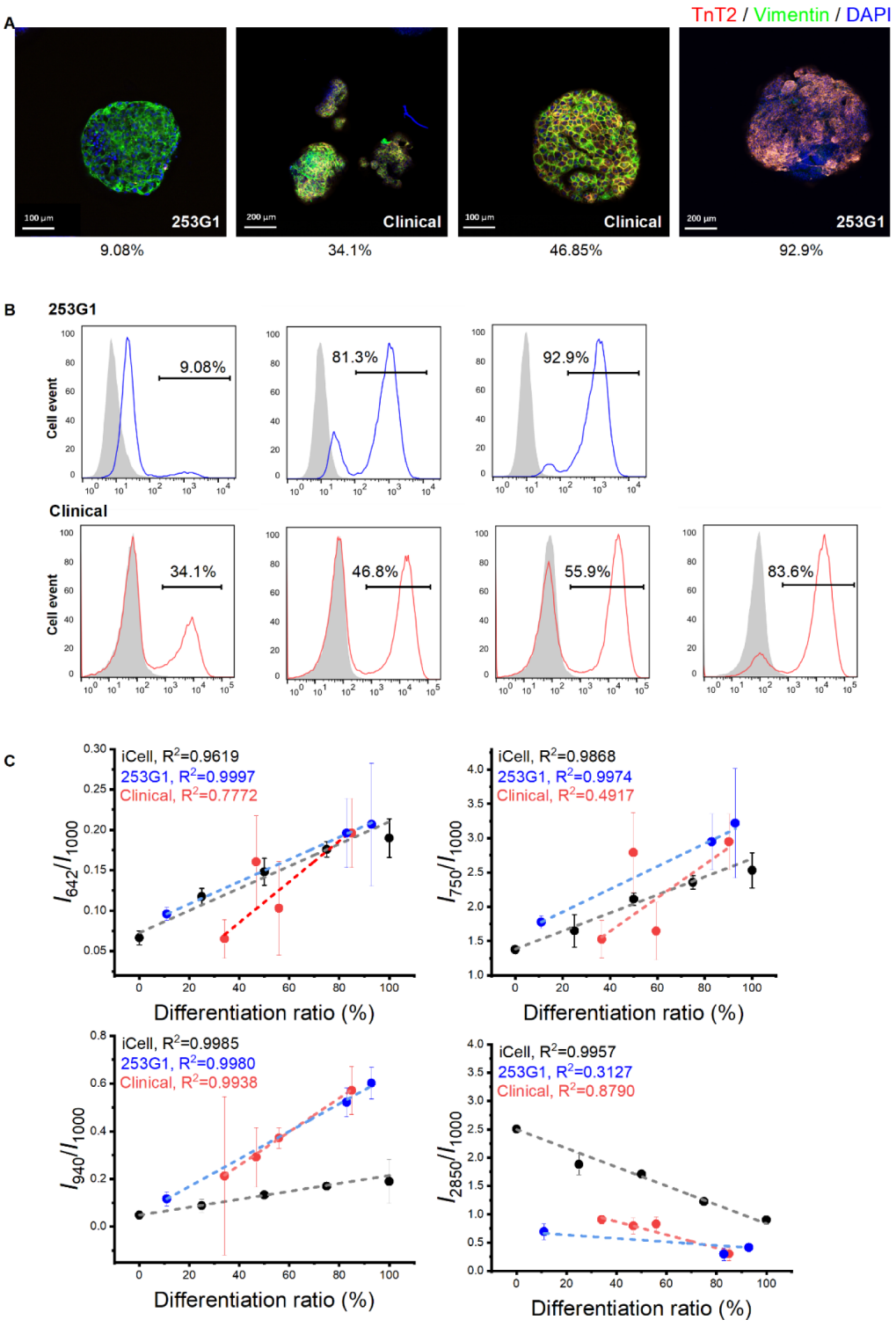

Figure 2. Raman observation on human induced pluripotent stem cells (hiPSCs) differentiated cardiac spheroids. (A) Representative confocal images of hiPSC differentiated cardiac spheroids. The spheroids were stained with anti-TnT2, anti-vimentin and DAPI. The TnT2 positive ratios obtained by fluorescence-activated cell sorting were illustrated in the bottom. (B) Representative flow cytometry data of cTnT-positive cells differentiated from hiPSCs (253G1 and clinical cell line: QHJI14s04) in different experimental batches. (C) Quantitative analysis of the Raman intensity at 642, 750, 940, and 2,850 cm^{-1} (mean ± SD, each point represents average value from 3 to 5 spheroids from one independent differentiation).

utility in distinguishing CMs from non-CMs in the hiPSC-derived mixture. Raman microscopy was also used to distinguish the CMs from the non-CMs,[14,15] with a reported specificity of 97% and a sensitivity of 96% for dissociated single CMs.[15] In addition, Brauchle et al. have shown that Raman can be employed to obtain biochemical fingerprints of atrial and ventricular CMs differentiated from embryonic stem (ES) cells, while also distinguishing fibroblasts from CMs.[16] However, most of these reports are confined to analyses at the single-cell level. Notably, there is a lack of reports comparing Raman data

https://doi.org/10.1021/acs.analchem.4c03871
Anal. Chem. 2024, 96, 15765−15772

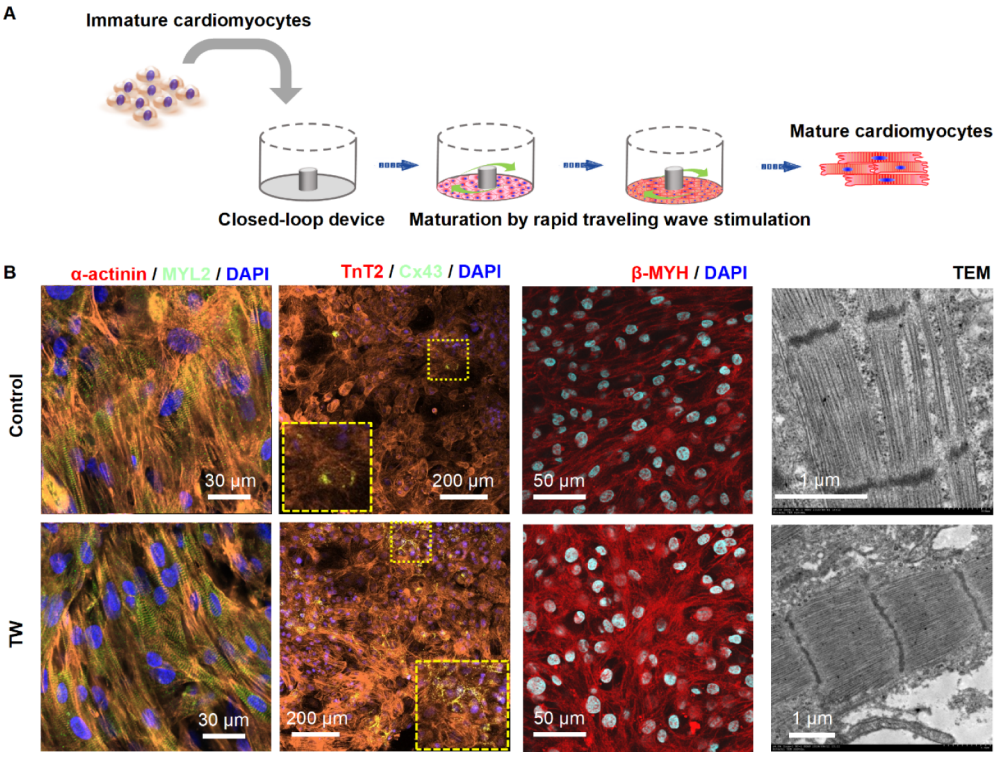

Figure 3. Rapid pacing of traveling wave promote maturation of hiPSC-derived cardiomyocytes (CMs). (A) Schematic and image describing the cell plating and traveling wave origination in the close-loop device. (B) Representative confocal images of cardiac tissue with or without traveling wave (TW) on day 14. CMs were stained with anti-α-actinin, anti-MYL2, anti-TnT2, anti-Cx43, anti-β-MHC, and DAPI. Transmission electron microscopy (TEM) analysis of cardiac tissue was performed for both the TW training and control groups on day 14.

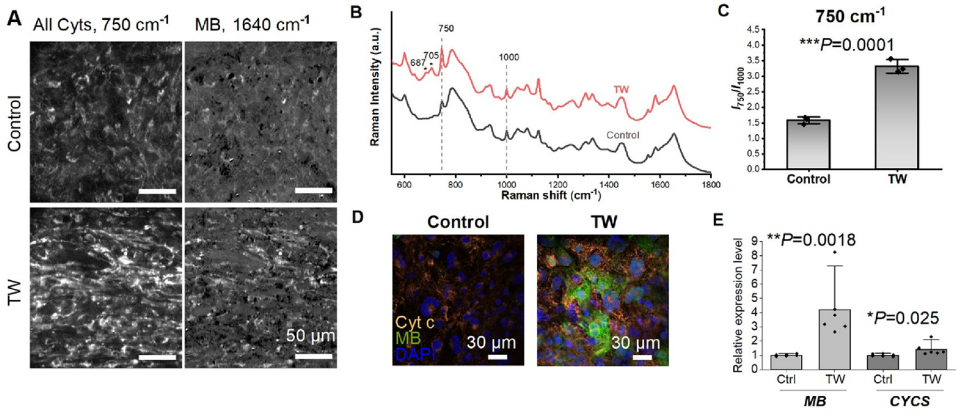

Figure 4. Raman analysis of hiPSC-derived cardiac tissue at different maturation levels. (A) Reconstructed Raman images at 750 and 1,640 cm^{-1}. (B) Comparison of average Raman signal for hiPSC-derived cardiac tissue with (TW) or without (Control) TW training. (C) Quantitative analysis of the Raman intensity at 750 cm^{-1} (mean ± SD, n = 3 biologically independent samples, *p < 0.05, **p < 0.01, ***p < 0.001). (D) Representative confocal images of hiPSC-derived cardiac tissue with different maturation level on day 14. The cells were stained with anti with anti-Cyt c, anti-MB, and DAPI. (E) Relative gene expression of Cyt-c (*CYCS*) and *MB*. (mean ± SD, n = 6 biologically independent samples, *p < 0.05, **p < 0.01).

with results from molecular biology assays, such as flow cytometry, immunostaining, and genetic analysis, particularly regarding CMs with varying differentiation efficiencies and purities. Additionally, although the potential of Raman spectroscopy for assessing CMs has been demonstrated, specific markers for evaluating CMs have yet to be identified.

In this study, we employed line-illumination Raman microscopy to directly observe 3D cardiac tissue, enabling the acquisition of several hundred spectra with a single exposure. The spatial resolution for visualizing living cells is comparable to that of laser scanning confocal microscopy. Reference samples were prepared by mixing commercially available iCell CMs and fibroblasts at different ratios in a v-bottom 96-well plate. Genetic and immunostaining analyses were utilized to confirm the content of iCell/fibroblast spheroids. Notably, Raman microscopy revealed a significant trend in iCell/fibroblast spheroids with different mixing ratios. To further validate these results, the Raman spectrum of 3D spheroids differentiated from iPSCs exhibited a similar trend to the reference samples, as confirmed using flow cytometry. Among these peaks, specific markers such as cytochrome *c* and

https://doi.org/10.1021/acs.analchem.4c03871
Anal. Chem. 2024, 96, 15765−15772

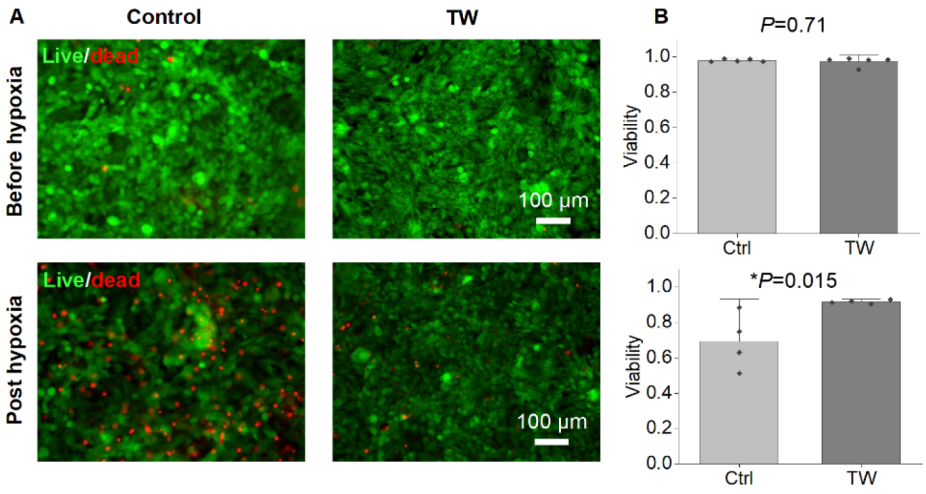

Figure 5. Mature CMs showed enhanced survival post hypoxia. (A) Representative images for live/dead staining on hiPSC-derived cardiac tissue at different maturation level before and after hypoxia culture (5% oxygen) for 5 d. (B) Quantitative analysis of the viability for both groups (mean ± SD, n = 4 biologically independent samples, *p < 0.05).

myoglobin were identified, which may serve as potential markers for quantifying CMs purity.

The iPSC-CMs tend to display an immature phenotype compared with adult CMs, in terms of sarcomere structure, electrophysiology, contractile function, and calcium-handling properties.[17] These differences may impede their application in disease modeling and regenerative therapy. Shen et al. utilized Raman analysis to compare hESC-derived CMs at various maturation stages, revealing distinct bands and indicating that the trained CMs resemble fetal CMs more closely than the control CMs.[18] However, due to the use of a 785 nm laser, the information regarding cytochromes was not revealed. In this study, we employed line-illumination Raman microscopy at an excitation wavelenght of 532 nm to observe CMs with different maturation levels generated using our previously developed traveling wave-based method.[19−21] This approach revealed significantly distinct Raman spectra and enabled the visualization of living cells among different groups. Notably, the expression of cytochrome c and myoglobin was higher in CMs with advanced maturation levels compared with control group. We demonstrated that cytochrome c and myoglobin can serve as markers for noninvasively assessing the purity and maturation of CMs through Raman-based measurements.

RESULTS AND DISCUSSION

Raman Spectra of Spheroid Mixture of iCell and Fibroblast at Different Ratios. The spheroids made by using different ratios of CMs and fibroblasts were subjected to immunostaining, RT-PCR, and Raman evaluation (Figure 1). Immunostaining data confirmed changes in composition within the iCell/fibroblast spheroids across different mixture ratios. Lower expression levels of cytochrome c, TnT2, α-actinin, and myoglobin were observed in groups with lower CMs content (Figure 1A), a trend corroborated by the RT-PCR data (Figure 1B). Raman spectra of these samples revealed significant linear decreases in Raman shift at 642 cm^{-1} (cytochrome c) and 750 cm^{-1} (all cytochromes) as the CM content decreased (Figure 1C−E). Additionally, Raman peaks at 940 cm^{-1} and 1,640 cm^{-1} indicated reduced glycogen and myoglobin (MB) content, respectively. Increased lipid droplets (2,850 cm^{-1}) were observed in groups with lower CMs ratio.

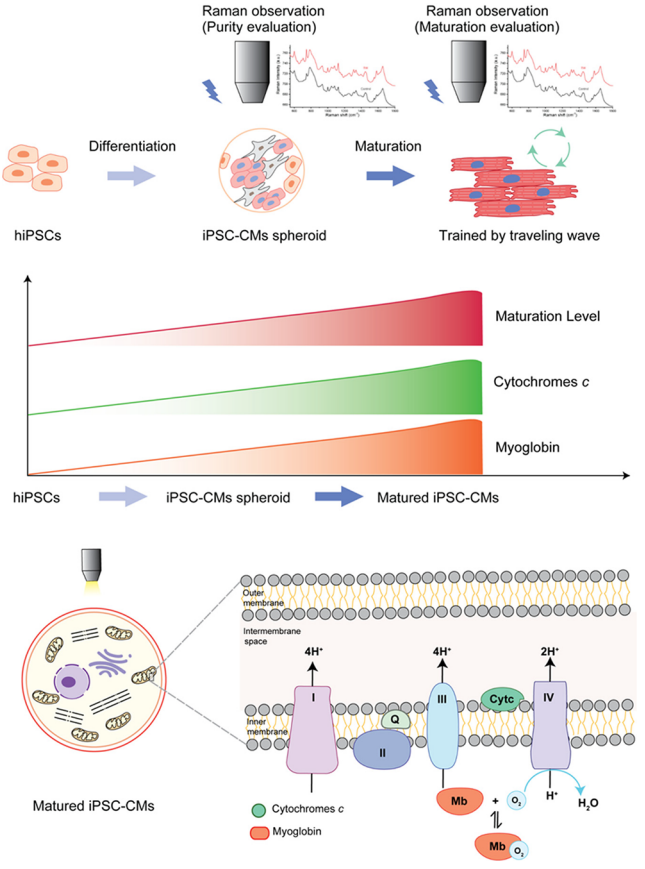

Figure 6. Cytochrome c and myoglobin content increase during the iPSC differentiation into CMs and their maturation.

Raman Microscopy for Analyzing the Efficiency of Differentiation in Live Cardiac Spheroids During Differentiation. In addition to the Raman observation of iCell/fibroblast spheroids, we further analyzed the Raman spectra of CM spheroids differentiated from two hiPSC cell lines (research grade: 253G1 and clinical grade: QHJI14s04, Supplementary Figures 1 and 2). The CMs with different TnT2 positive ratios were used for Raman microscopy. The immunostaining and flow cytometry data confirmed the

https://doi.org/10.1021/acs.analchem.4c03871
Anal. Chem. 2024, 96, 15765−15772

various contents of hiPSC-derived CM spheroids (Figure 2A,B). Spheroids in the same production lots were used for Raman spectroscopy analysis (Figure 2C). Linear increases were observed in both 253G1 (R^2 = 0.9997) and QHJI14s04 (R^2 = 0.7772) groups in Raman shift at 642 cm^{-1}, similar to the iCell group (R^2 = 0.9619), indicating an increased cytochrome *c* content in the group with a higher TnT2 positive ratio. Additionally, the Raman shift at 750 cm^{-1} (all cytochromes) showed a linear increase in the 253G1 group (R^2 = 0.9974), but not in the QHJI14s04 group (R^2 = 0.4917), in which all the data points were distributed around the iCell trendline (R^2 = 0.9868). The QHJI14s04 group exhibited a significant linear increase in glycogen (940 cm^{-1}, R^2 = 0.9938) and a decrease in lipid contents (2,850 cm^{-1}, R^2 = 0.879) respectively, correlating with a higher TnT2 positive ratio, similar to the findings in the iCell group (940 cm^{-1}: R^2 = 0.9985; 2,850 cm^{-1}: R^2 = 0.9957). However, this trend exists only in glycogen (940 cm^{-1}: R^2 = 0.998), but not in lipid (2,850 cm^{-1}: 0.3127) for the 253G1 cell line. These data indicate that although there is a variation in the Raman profiles among different cell lines, certain Raman spectra, such as that of cytochrome *c*, may be used as a universal marker for assessing the CM content in the hiPSC-derived mixture.

CMs constitute approximately 30−40% of the cell numbers in the heart, with the majority of the remaining cells being nonmyocytes, primarily comprised of fibroblasts.[22] Similarly, the hiPSC-derived CMs mixture predominantly exhibits positivity for the cardiac marker troponin T (TnT2), while the non-CMs predominantly express the fibroblast marker vimentin (>70%), the smooth muscle marker (∼30%), and to a lesser extent, the endothelial cell marker CD31 (∼2%).[23] The CMs derived from hiPSCs may continue beating for the long-term and consume much more oxygen than non-CMs in the heart.[24,25] MB, an essential oxygen-binding protein present exclusively in muscle cells, plays a critical role in providing energy through oxygen storage and transportation. Additionally, cytochrome is a component of the mitochondrial electron transport chain involved in ATP production for cardiac cell contraction.[26] These align well with the linear relationship observed between MB and cytochrome *c*, as well as the CM content in the hiPSC-derived mixture.

Although there is variations among iPSC-CM spheroids, even from the same production batch, which may cause significant differences during the Raman evaluation (Figure 2C), increasing the number of sampled spheroids in the assay may mitigate this variation in the data and could also impose higher throughput requirements. The scanning speed for current Raman observations remains insufficient, thus limiting assay throughput. To address this limitation, our future efforts will concentrate on enhancing scanning speed, increasing scanning points, optimizing spheroid arrangement, and implementing more efficient analysis. We have recently developed a 96-well-plate-based Raman system for the simultaneous analysis of multiple spheroids[27] and upgraded single-line illumination to multiline illumination.[28] These enhanced systems could be leveraged for future large-scale analysis of hiPSC-derived cardiac tissue, potentially increasing throughput by two to three orders of magnitude compared to the current system.

Preparing Mature hiPSC-Derived CM Tissue by Using Traveling Wave Promotion. We previously developed a spontaneously originating traveling wave (TW)-based method for promoting the maturation of hiPSC-derived CMs (Figure 3A).[19,21] After a 2-week training period with TW, the CMs exhibited improved sarcomeric organization, upregulated expression of cardiac-specific genes, enhanced Ca^{2+} handling properties, increased oxygen consumption rate, and enhanced contractile force. In the present study, we cultured mature hiPSC-derived cardiac tissues in a monolayer formation for observation using Raman spectroscopy (Figure 3A). The mature TW group demonstrated significantly increased expression of the gap junction marker (Cx43), and the mature CMs marker (*α*-actinin, MYL2, *β*-myosin heavy chain [*β*-MHC]). Additionally, electron microscopy revealed that the CMs in the TW group exhibited larger sarcomere bundles and well-defined Z disks, I-bands, and myofibrils compared to those in the control group (Figure 3B).

Raman Microscopy for Analyzing Cardiac Tissue with Different Maturation Levels. We utilized line-illumination Raman microscopy to characterize both the mature TW group and the control group. The TW group exhibited increased expression (as depicted in Figure 4A−C) of cytochromes (750 cm^{-1}) and MB (1,640 cm^{-1}). The heightened expression of cytochrome *c* and MB was validated through both immunostaining and reverse transcription polymerase chain reaction (RT-PCR) (Figure 4D,E). Maturation of hiPSC-derived cardiac tissue was associated with enhanced cytochrome *c* activity.[29−31] Moreover, hearts rich in MB outperformed those with lower MB levels under hypoxic conditions,[32] and animals acclimated to low-oxygen environments exhibited increased concentrations of MB in skeletal or cardiac muscle.[33,34] We further assessed the survival rates under hypoxic conditions for both groups with varying levels of MB expression (Figure 5). While there was no discernible difference in viability between the TW and control groups prior to hypoxic culture, following 5 days of hypoxic culture, the TW group displayed viability significantly greater than that of the control group (Figure 5). This suggests that the heightened expression of MB may have augmented the survival of TW CMs due to (1) enhancement of the cells' ability to acquire oxygen through MB;[32] and (2) cardio-protective effects of MB.[35]

The maturation level of iPSC-derived CMs is crucial for their clinical applications and disease modeling.[17,36] CM maturity can be assessed using various molecular biology techniques such as immunostaining, RT-PCR, and transmission electron microscopy (TEM). However, these methods require sample treatment, rendering the cells unusable for further applications after evaluation. Raman microscopy, distinguished by its marker-free and nondestructive nature, necessitates no specific sample treatment. In a prior investigation, significant differences in Raman spectra were observed among hESC-derived CMs at varying maturation stages.[18] Nonetheless, only a limited number of Raman peaks have been reported to be associated with CM maturation. In addition, the Raman spectra have been used for evaluating amount of MB and cytochrome *c* in the cardiomyocytes,[37,38] through which cellular function such as mitochondrial respiration could be monitored.[39] In this study, we identified MB and cytochrome *c* as indicators of CM maturation, both crucial for oxygen transport and ATP generation, which are fundamental activities in muscle cells. Oxygen consumption rates vary substantially among different cell types,[24,25,40] and several previous studies, including our own, have noted that iPSC-derived CMs exhibit greater oxygen consumption when they have undergone higher levels of maturation compared to

https://doi.org/10.1021/acs.analchem.4c03871
Anal. Chem. 2024, 96, 15765−15772

their immature counterparts.[19,41−43] Furthermore, the rate of oxygen consumption, which correlates with ATP synthesis in CMs, is linked to the fraction of cytochrome present.[44,45] MB functions as both a reservoir and transporter of oxygen to support mitochondrial respiration.[46,47] The expression profile of MB is positively associated with the maturation of cardiac lineage cells,[48] including hiPSC-derived CMs matured by long-term culture.[49] Mature cardiac tissue typically exhibits elevated cytochrome *c* activity[29−31] and MB expression.[19,48,50] Taken together, these findings suggest that Raman microscopy could serve as an ideal tool for assessing the maturation and purity of hiPSC-derived cardiac tissue (Figure 6).

CONCLUSIONS

In summary, label-free Raman microscopy has been employed to evaluate hiPSC-derived cardiac tissue. The obtained Raman spectroscopy data reveal a direct correlation between the Raman peaks associated with cytochrome *c* and myoglobin and the purity of hiPSC-derived CM spheroids. Furthermore, a comparison of hiPSC-CMs at different maturation stages shows that the cytochrome *c* and myoglobin peaks also positively correlate with CM maturation. These findings suggest that Raman microscopy holds potential as a novel tool for real-time assessment of both the purity and maturation status of hiPSC-derived cardiac tissue.

ASSOCIATED CONTENT

Supporting Information

The Supporting Information is available free of charge at https://pubs.acs.org/doi/10.1021/acs.analchem.4c03871.

Methods, the preparation of iCell/fibroblast spheroids, preparation of hiPSCs and differentiation into CMs, flow cytometry, promoting maturation ofhiPSC-CM tissue by using traveling wave, immunostaining and imaging, live/dead assay, transmission electronmicroscopy (TEM), etc. (PDF)

AUTHOR INFORMATION

Corresponding Authors

Junjun Li − *Laboratory of Nanophotonics, Department of Applied Physics, Osaka University, Suita, Osaka 565-0871, Japan; Frontier of Regenerative Medicine, Osaka University Graduate School of Medicine, Osaka, Suita 565-0871, Japan;* orcid.org/0000-0002-7473-4918; Email: lijunjun@ap.eng.osaka-u.ac.jp

Katsumasa Fujita − *Laboratory of Nanophotonics, Department of Applied Physics, Osaka University, Suita, Osaka 565-0871, Japan; Advanced Photonics and Biosensing Open Innovation Laboratory, National Institute of Advanced Industrial Science and Technology (AIST), Suita, Osaka 565-0871, Japan;* orcid.org/0000-0002-2284-375X; Email: fujita@ap.eng.osaka-u.ac.jp

Li Liu − *Laboratory of Nanophotonics, Department of Applied Physics, Osaka University, Suita, Osaka 565-0871, Japan; Frontier of Regenerative Medicine, Osaka University Graduate School of Medicine, Osaka, Suita 565-0871, Japan;* Email: liuli@ap.eng.osaka-u.ac.jp

Authors

Menglu Li − *Laboratory of Nanophotonics, Department of Applied Physics, Osaka University, Suita, Osaka 565-0871, Japan;* Present Address: Shenzhen Medical Academy of Research and Translation, Shenzhen 518107, China; orcid.org/0000-0003-2223-1881

Yasunori Nawa − *Laboratory of Nanophotonics, Department of Applied Physics, Osaka University, Suita, Osaka 565-0871, Japan; Advanced Photonics and Biosensing Open Innovation Laboratory, National Institute of Advanced Industrial Science and Technology (AIST), Suita, Osaka 565-0871, Japan*

Yuting Liu − *Department of Cardiovascular Surgery, Osaka University Graduate School of Medicine, Osaka, Suita 565-0871, Japan*

Kazuki Bando − *Advanced Photonics and Biosensing Open Innovation Laboratory, National Institute of Advanced Industrial Science and Technology (AIST), Suita, Osaka 565-0871, Japan*

Ying Hua − *Department of Cardiovascular Surgery, Osaka University Graduate School of Medicine, Osaka, Suita 565-0871, Japan*

Lifu Sun − *Department of Cardiovascular Surgery, Osaka University Graduate School of Medicine, Osaka, Suita 565-0871, Japan*

Satoshi Fujita − *Advanced Photonics and Biosensing Open Innovation Laboratory, National Institute of Advanced Industrial Science and Technology (AIST), Suita, Osaka 565-0871, Japan*

Yoshiki Sawa − *Department of Cardiovascular Surgery, Osaka Police Hospital, Osaka 543-0035, Japan; Cuorips Inc., Chuo City, Tokyo 103-0023, Japan*

Complete contact information is available at: https://pubs.acs.org/10.1021/acs.analchem.4c03871

Author Contributions

○J.L. and M.L. contributed equally. J.L., M.L., Y.N., K.F., and L.L. conceived the concept; J.L., M.L., and Y.N. designed the experiments with the help of Y.S., K.F., and L.L.; J.L., M.L., Y.N., Y.L., K.B., Y.H., and L.S. performed the experiments; J.L., M.L., and Y.N. analyzed the data; Y.N. and S.F. provided tools for Raman measurement and analysis; Y.N. and M.L., carried out the optical alignment; J.L., M.L., K.F., and L.L. wrote the manuscript with input from all authors. All authors have read and agreed to submit the manuscript. All authors confirm their consent for publication.

Notes

The authors declare that they have not used artificial intelligence in this study.

The authors declare no competing financial interest.

ACKNOWLEDGMENTS

Funding was provided by the Japan Society for the Promotion of Science (JSPS; 22K12801, 22H03157). This research was also supported by the JST COI-NEXT under Grant JPMJPF2009.

REFERENCES

(1) Miyagawa, S.; Kainuma, S.; Kawamura, T.; Suzuki, K.; Ito, Y.; Iseoka, H.; Ito, E.; Takeda, M.; Sasai, M.; Mochizuki-Oda, N.; et al. *Front. Cardiovasc. Med.* **2022**, *9*, 950829.

(2) Li, J.; Liu, L.; Zhang, J.; Qu, X.; Kawamura, T.; Miyagawa, S.; Sawa, Y. *Bioengineering* **2022**, *9* (11), 605.

(3) Kawamura, T.; Ito, Y.; Ito, E.; Takeda, M.; Mikami, T.; Taguchi, T.; Mochizuki-Oda, N.; Sasai, M.; Shimamoto, T.; Nitta, Y. *Front. Cardiovasc. Med.* **2023**, *10*, 1182209.

(4) Li, J.; Minami, I.; Shiozaki, M.; Yu, L.; Yajima, S.; Miyagawa, S.; Shiba, Y.; Morone, N.; Fukushima, S.; Yoshioka, M. *Stem Cell Rep.* **2017**, *9* (5), 1546−1559.
(5) Blinova, K.; Dang, Q.; Millard, D.; Smith, G.; Pierson, J.; Guo, L.; Brock, M.; Lu, H. R.; Kraushaar, U.; Zeng, H.; Shi, H.; Zhang, X.; Sawada, K.; Osada, T.; Kanda, Y.; Sekino, Y.; Pang, L.; Feaster, T. K.; Kettenhofen, R.; Stockbridge, N.; Strauss, D. G.; Gintant, G. *Cell Rep.* **2018**, *24* (13), 3582−3592.
(6) Goversen, B.; van der Heyden, M. A.; van Veen, T. A.; de Boer, T. P. *Pharmacol. Ther.* **2018**, *183*, 127−136.
(7) Ogawa, M.; Harada, Y.; Yamaoka, Y.; Fujita, K.; Yaku, H.; Takamatsu, T. *Biochem. Biophys. Res. Commun.* **2009**, *382* (2), 370−374.
(8) Li, M.; Ueyama-Toba, Y.; Lindley, M.; Kongklad, G.; Nawa, Y.; Kumamoto, Y.; Ishida, S.; Kanda, Y.; Fujita, S.; Mizuguchi, H. *Anal. Chem.* **2023**, *95*, 9252−9262.
(9) Li, M.; Nawa, Y.; Ishida, S.; Kanda, Y.; Fujita, S.; Fujita, K. *Commun. Biol.* **2022**, *5* (1), 778.
(10) Brauchle, E.; Thude, S.; Brucker, S. Y.; Schenke-Layland, K. *Sci. Rep.* **2014**, *4* (1), 4698.
(11) Kar, S.; Jaswandkar, S. V.; Katti, K. S.; Kang, J. W.; So, P. T.; Paulmurugan, R.; Liepmann, D.; Venkatesan, R.; Katti, D. R. *Sci. Rep.* **2022**, *12* (1), 8050.
(12) Hsu, C.-C.; Xu, J.; Brinkhof, B.; Wang, H.; Cui, Z.; Huang, W. E.; Ye, H. *Proc. Natl. Acad. Sci. U. S. A.* **2020**, *117* (31), 18412−18423.
(13) Pascut, F. C.; Goh, H. T.; Welch, N.; Buttery, L. D.; Denning, C.; Notingher, I. *Biophys. J.* **2011**, *100* (1), 251−259.
(14) Pascut, F. C.; Kalra, S.; George, V.; Welch, N.; Denning, C.; Notingher, I. *Biochimica Et Biophysica Acta (BBA)-General Subjects* **2013**, *1830* (6), 3517−3524.
(15) Chan, J. W.; Lieu, D. K.; Huser, T.; Li, R. A. *Anal. Chem.* **2009**, *81* (4), 1324−1331.
(16) Brauchle, E.; Knopf, A.; Bauer, H.; Shen, N.; Linder, S.; Monaghan, M. G.; Ellwanger, K.; Layland, S. L.; Brucker, S. Y.; Nsair, A. *Stem Cell Rep.* **2016**, *6* (2), 188−199.
(17) Li, J.; Hua, Y.; Miyagawa, S.; Zhang, J.; Li, L.; Liu, L.; Sawa, Y. *Int. J. Mol. Sci.* **2020**, *21* (23), 8893.
(18) Shen, N.; Knopf, A.; Westendorf, C.; Kraushaar, U.; Riedl, J.; Bauer, H.; Pöschel, S.; Layland, S. L.; Holeiter, M.; Knolle, S.; Brauchle, E.; Nsair, A.; Hinderer, S.; Schenke-Layland, K. *Stem Cell Rep.* **2017**, *9* (1), 122−135.
(19) Li, J.; Zhang, L.; Yu, L.; Minami, I.; Miyagawa, S.; Hörning, M.; Dong, J.; Qiao, J.; Qu, X.; Hua, Y. *Commun. Biol.* **2020**, *3* (1), 122.
(20) Zhang, L.; Li, J.; Liu, L.; Tang, C. *Sci. Rep.* **2020**, *10* (1), 2984.
(21) Li, J.; Hua, Y.; Liu, Y.; Qu, X.; Zhang, J.; Ishida, M.; Yoshida, N.; Tabata, A.; Miyoshi, H.; Shiba, M.; Higo, S.; Sougawa, N.; Takeda, M.; Kawamura, T.; Matsuura, R.; Okuzaki, D.; Toyofuku, T.; Sawa, Y.; Liu, L.; Miyagawa, S. *iScience* **2024**, *27* (2), 108992.
(22) Camelliti, P.; Borg, T. K.; Kohl, P. *Cardiovasc. Res.* **2005**, *65* (1), 40−51.
(23) Miyagawa, S.; Kawamura, T.; Ito, E.; Takeda, M.; Iseoka, H.; Yokoyama, J.; Harada, A.; Mochizuki-Oda, N.; Imanishi-Ochi, Y.; Li, J.; et al. *bioRxiv* **2021**.
(24) Sekine, K.; Kagawa, Y.; Maeyama, E.; Ota, H.; Haraguchi, Y.; Matsuura, K.; Shimizu, T. *Biochem. Biophys. Res. Commun.* **2014**, *452* (3), 834−839.
(25) Wagner, B. A.; Venkataraman, S.; Buettner, G. R. *Free Radical Biol. Med.* **2011**, *51* (3), 700−712.
(26) Almohammedi, A.; Kapetanaki, S.; Wood, B. R.; Raven, E. L.; Storey, N.; Hudson, A. J. *J. R. Soc., Interface* **2015**, *12* (105), 20141339.
(27) Liao, H.-X.; Bando, K.; Li, M.; Fujita, K. *Anal. Chem.* **2023**, *95* (39), 14616−14623.
(28) Mochizuki, K.; Kumamoto, Y.; Maeda, S.; Tanuma, M.; Kasai, A.; Takemura, M.; Harada, Y.; Hashimoto, H.; Tanaka, H.; Smith, N. I. *Biomed. Opt. Express* **2023**, *14* (3), 1015−1026.
(29) Shadrin, I. Y.; Allen, B. W.; Qian, Y.; Jackman, C. P.; Carlson, A. L.; Juhas, M. E.; Bursac, N. *Nat. Commun.* **2017**, *8* (1), 1825.
(30) Guo, Y.; Pu, W. T. *Circ. Res.* **2020**, *126* (8), 1086−1106.
(31) Chirico, N.; Kessler, E. L.; Maas, R. G.; Fang, J.; Qin, J.; Dokter, I.; Daniels, M.; Šarić, T.; Neef, K.; Buikema, J.-W. *Stem Cell Res. Ther.* **2022**, *13* (1), 531.
(32) Driedzic, W. R.; Stewart, J. M.; Scott, D. L. *J. Mol. Cell. Cardiol.* **1982**, *14* (11), 673−677.
(33) Jaspers, R. T.; Testerink, J.; Della Gaspera, B.; Chanoine, C.; Bagowski, C. P.; van der Laarse, W. J. *Biology Open* **2014**, *3* (8), 718−727.
(34) De Miranda, M. A., Jr; Schlater, A. E.; Green, T. L.; Kanatous, S. B. *J. Exp. Biol.* **2012**, *215* (5), 806−813.
(35) Hendgen-Cotta, U. B.; Kelm, M.; Rassaf, T. *Free Radical Biol. Med.* **2014**, *73*, 252−259.
(36) Khanna, A.; Oropeza, B. P.; Huang, N. F. *J. Biomed Mater. Res. A* **2024**, *112*, 512−523.
(37) Brazhe, N. A.; Treiman, M.; Brazhe, A. R.; Find, N. L.; Maksimov, G. V.; Sosnovtseva, O. V. *PLoS One* **2012**, *7* (9), No. e41990.
(38) El-Said, W. A.; Fouad, D. M.; El-Safty, S. A. *Sens. Actuators, B* **2016**, *228*, 401−409.
(39) Ohira, S.; Tanaka, H.; Harada, Y.; Minamikawa, T.; Kumamoto, Y.; Matoba, S.; Yaku, H.; Takamatsu, T. *Sci. Rep.* **2017**, *7* (1), 42401.
(40) Zhao, J.; Gao, J.-L.; Zhu, J.-X.; Zhu, H.-B.; Peng, X.; Jiang, M.; Fu, Y.; Xu, J.; Mao, X.-H.; Hu, N. *Basic Res. Cardiol.* **2019**, *114*, 12.
(41) Ronaldson-Bouchard, K.; Ma, S. P.; Yeager, K.; Chen, T.; Song, L.; Sirabella, D.; Morikawa, K.; Teles, D.; Yazawa, M.; Vunjak-Novakovic, G. *Nature* **2018**, *556* (7700), 239.
(42) Yoshida, S.; Miyagawa, S.; Fukushima, S.; Kawamura, T.; Kashiyama, N.; Ohashi, F.; Toyofuku, T.; Toda, K.; Sawa, Y. *Mol. Ther.* **2018**, *26* (11), 2681−2695.
(43) Nunes, S. S.; Miklas, J. W.; Liu, J.; Aschar-Sobbi, R.; Xiao, Y.; Zhang, B.; Jiang, J.; Massé, S.; Gagliardi, M.; Hsieh, A.; Thavandiran, N.; Laflamme, M. A.; Nanthakumar, K.; Gross, G. J.; Thavandiran, N.; Laflamme, M. A.; Nanthakumar, K.; Gross, G. J. *Nat. Methods* **2013**, *10* (8), 781−787.
(44) Wilson, D. F.; Harrison, D. K.; Vinogradov, A. *J. Appl. Physiol.* **2014**, *117* (12), 1424−1430.
(45) Ow, Y.-L. P.; Green, D. R.; Hao, Z.; Mak, T. W. *Nat. Rev. Mol. Cell Biol.* **2008**, *9* (7), 532−542.
(46) Wittenberg, B. A.; Wittenberg, J. B. *Proc. Natl. Acad. Sci. U. S. A.* **1987**, *84* (21), 7503−7507.
(47) Wittenberg, B.; Wittenberg, J.; Caldwell, P. *J. Biol. Chem.* **1975**, *250* (23), 9038−9043.
(48) Hsieh, M.-Y. A. High Gradient Labelling-Free Isolation of Cardiomyocytes from Heterogeneous Populations. Ph.D. Thesis, University of Toronto, Toronto, ON, Canada, 2016.
(49) Cai, W.; Zhang, J.; Lange, W. J. D.; Gregorich, Z. R.; Karp, H.; Farrell, E. T.; Mitchell, S. D.; Tucholski, T.; Lin, Z.; Biermann, M.; McIlwain, S. J.; Ralphe, J. C.; Kamp, T. J.; Ge, Y. *Circ. Res.* **2019**, *125* (11), 936−953.
(50) Kanatous, S. B.; Mammen, P. P. *J. Exp. Biol.* **2010**, *213* (16), 2741−2747.

https://doi.org/10.1021/acs.analchem.4c03871
Anal. Chem. 2024, 96, 15765−15772